Available online at www.sciencedirect.com

SciVerse ScienceDirect

Ceramics International 38 (2012) 2701–2709

CERAMICS INTERNATIONAL

www.elsevier.com/locate/ceramint

Formulation and preparation of low-concentrated yttria colloidal dispersions

K. Verhiest [a,d,e,*], S. Mullens [b], N. De Wispelaere [c], S. Claessens [c], A. DeBremaecker [d], K. Verbeken [e], Y. Houbaert [e]

[a] ArcelorMittal Gent, Hot Strip Mill Department, J. Kennedylaan 51, 9042 Gent, Belgium
[b] Flemish Institute for Technological Research, VITO, Materials Technology, Boeretang 200, 2400 Mol, Belgium
[c] ArcelorMittal Research Industry Gent, OCAS, J. Kennedylaan 3, 9060 Zelzate, Belgium
[d] Belgian Nuclear Research Centre, SCK CEN, Boeretang 200, 2400 Mol, Belgium
[e] Ghent University, UGent, Department of Materials Science and Engineering (DMSE), Technologiepark 903, 9052 Ghent, Belgium

Received 8 February 2011; received in revised form 11 November 2011; accepted 12 November 2011
Available online 22 November 2011

Abstract

High-temperature creep resistant steels for nuclear applications consist of a steel matrix reinforced with a dispersion of nano-sized refractory ceramic oxide particles, e.g. yttria (Y_2O_3). In this study, the formulation and preparation of low-loaded (2, 3 and 4 vol.%) Y_2O_3 colloidal dispersions for its possible application as suspension precursor in the production of high-temperature creep resistant steels is discussed. The final end product is formulated as a low-concentrated and low-viscous colloidal suspension consisting of non-agglomerated Y_2O_3 nano-particles in the (sub)-100 nm range.

The spherical as-received and submicron agglomerated powder necessitates ball-mill processing in order to reduce the as-received size distribution down to nano-level. A comparative study on the desagglomeration of Y_2O_3 nano-powder using conventional planetary ball-milling or nano-milling technology has been done. Formulation of stable colloidal suspensions by screening suitable dispersants has led to the selection of one specific dispersant for this application, Calgon N. Suspension characterization by the determination of particle size distribution (PSD), ζ-potential measurements, colloidal suspension visualization using transmission electron microscopy (TEM), rheology and suspension life-time is discussed in this paper.

Keywords: E. Nuclear applications; Planetary ball-milling; Nano-milling; Colloidal suspension

1. Introduction

Nano-structured materials are considered of high interest in many technical domains, as they exhibit interesting physical and mechanical properties. Rare-earth oxide ceramics proof their usefulness as refractory component in many industrial domains such as high-energy permanent magnets, solid electrolytes for fuel cells, photoluminescency and as catalyst materials [1–6]. Another example are the advanced creep and corrosion resistant steels, which are well-known for their high-temperature creep resistance required for nuclear applications. They typically consist of a matrix structure reinforced by a dispersion of nano-sized rare-earth metal oxides, such as yttrium oxide (Y_2O_3) [7]. For this type of application, in which the nano-particles dispersion in the matrix is crucial for the final mechanical properties, the formulation of suspensions with a non-agglomerated particle size distribution (PSD) is a key issue [7,8]. To implement them as subcomponent in a steel structure, ceramic powders are mostly processed in the 'dry' condition. Typical dry pressing methods used in powder metallurgical processing are hot and cold isostatic pressing (HIP and CIP), in which refractory nano-powders are often pre-mixed with alloy powders and consequently CIPped to form the steel alloy [9,10]. Alternatively, a new route can be searched towards wet forming methods, in which ceramic powders are processed as a slurry (low to high viscous suspensions). Colloidal processing has shown its potential in many high performance domains allowing to facilitate the technical implementation of ceramics

* Corresponding author at: ArcelorMittal Gent, Hot Strip Mill Department, J. Kennedylaan 51, 9042 Gent, Belgium.
Tel.: +32 9 347 23 10; fax: +32 9 347 49 78.
E-mail address: Katelijne.Verhiest@ArcelorMittal.com (K. Verhiest).

0272-8842/$36.00
doi:10.1016/j.ceramint.2011.11.038

Table 1
Main physical properties of the dispersing agents used.

Dispersant	Lopon 890	Calgon N	9056 KV	Dolapix CA	Darvan C
Active pH area (20 °C)	$pH_{(original)}$ = 8–9	$pH_{(1\%)}$ = 7.3–7.9	$pH_{(1\%)}$ = 2.5	8.5	8.5
Density (20 °C, g/cm^3)	1.3	(–)	1.06	1	1.10–1.12
Appearance	Liquid	White hygroscopic powder	Liquid	Viscous solution	Viscous solution
Optimal dosage formulation (wt.%)	0.2–0.5	0.05–0.15	(–)	(–)	(–)
Nomenclature ionic groups	Polyacrylate, sodium salt	Alkaline sodium polyphosphate of medium chain length, P_2O_5-content 63.5–65%	Acid phosphate ester	Synthetic polyelectrolyte; alkali free	Polymethacrylate, ammonium salt, ($COO^-NH_4^+$)-content 25%

Note: (–), product information not received from manufacturer; $pH_{(x)}$, pH value at suspension concentration x.

[11,12]. Various industrial applications of colloidal dispersions in pharmaceutical industry, cosmetics, household products and agrochemical science have proven the potential, workability and reliability of implementing colloidal formulations in the processing of nano-structured materials.

This work aims to study the formulation of low-concentrated and low-viscous (2, 3 and 4 vol.%) Y_2O_3 colloidal suspensions in terms of powder characterization, suspension preparation and characterization, with a special emphasis on powder size reduction. A difficulty to take into account when using ceramic oxides suspensions is the exothermal hydration reactivity of the rare-earth oxides with environmental moisture and dihydrogen oxide (H_2O) [13–15]. It must be stressed that the most difficult point in preparing aqueous Y_2O_3 nano-powder slurries, is the formulation of stable non-agglomerated Y_2O_3 suspensions because of the intrinsic fast aggregation of the nano-sized particles [13,15–17]. In order to obtain the final 'nano'-particle size distribution (PSD), a new desagglomeration technology, namely high tech nano-milling, is introduced within this work and compared to conventional planetary ball-milling. Mill speed, size and type of mill beads are evaluated. The formulation of the Y_2O_3 suspensions is optimized by ζ-potential measurements and rheology.

2. Materials and methods

2.1. Powder characterization

Spherical yttrium oxide (Y_2O_3) nano-powder (density ($\rho_{Y_2O_3}$) = 5.01 g/cm^3, specific surface area (SSA) = 23 ± 2 m^2/g) was used as starting material.[1] The particle size distribution (PSD) of the as-received powder was determined using a centrifugal particle sizing (CPS) disc centrifuge DC24000 (CPS Instruments, Inc.). As standard, a glucose gradient was injected at a rotation speed of 24.000 rpm. Spherical morphology of the as-received Y_2O_3 powder was verified using a field emission gun scanning electron microscopy (FEG-SEM) type JEOL JSM-6340F (JEOL Instruments).

[1] Data provided by the manufacturer. For reasons of confidentiality, producer and production process of the powder are not given in this study.

2.2. Suspension preparation

2.2.1. Dispersant selection

Different electrosteric dispersants suitable for dispersing rare-earth ceramics were screened. Table 1 summarizes the main physical properties of the dispersants used as provided by the manufacturer (Zschimmer & Schwarz GmbH and Co. KG, Germany). In this work, the paradigm of Lange is considered; no extra binders and plasticizers are added. Lange et al. proposed a new paradigm for powder processing, namely using powder with controlled particle size, morphology, purity, dispersion control and no binder addition [18,19].

Standard 0.6 vol.% yttria (Y_2O_3) suspensions in the as-received powder state were titrated with different dispersants (diluted to 1 wt.% in water) using a ZetaProbeFlowThrough-Sensor (Colloidal Dynamics, USA). In this study, suspension stabilization and particle re-agglomeration was prevented with the addition of functional dispersants inducing electrosteric stabilization. Electrosteric stabilization offers the advantage of a double stabilization compared to electrostatic stabilization, implying that not only the electrostatic interactions at the solid/liquid (S/L) interface are under control, but also steric repulsion is induced caused by the molecular architecture. Another reason to justify the addition of a functional dispersant is the reactivity of alkaline oxides towards H_2O and environmental moisture. Furthermore, besides dispersion stability with time, in our application, it is important to produce Y_2O_3 dispersions with a maximum concentration of particles per volume. Therefore, the most optimal dispersant was defined as the titrant inducing minimal dilution of the system and consequently restricting the level of organic matter added to the suspension.

2.2.2. Nano-milling versus conventional planetary milling

For ball-milling, yttria (Y_2O_3) suspensions with variation in solid loads (2, 3 and 4 vol.%) were prepared. To implement a particle break-up on the as-received powder, a comparative study of high-tech nano-milling versus conventional planetary ball-milling was done. Nano-milling was performed using the new nano-mill equipment, the Fritsch P-7 (Fritsch GmbH, Germany). Conventional planetary milling was performed with a regular Fritsch Pulverisette (Fritsch GmbH, Germany). The distinctive advantage of the nano-mill equipment compared to conventional planetary ball-milling equipment is its possibility to grind the material down to nano-level within reduced milling

Table 2
Process parameters used for planetary high-tech nano-milling and conventional planetary milling.

Milling characteristics	Conventional ball-milling	Nano-milling
Rotational speed max. (rpm)	626	1000
Sample volume (ml)	70	400
Sample vessel material	Polyamide	Stainless steel
Primary grinding media	YSZ (Ø 10 mm; 6.05 g/cm^3) YSZ (Ø 3 mm; 6.05 g/cm^3)	SS (Ø 1 mm; 7.8 g/cm^3)
Secondary grinding media	T91 (Ø 0.1 mm; 7.9 g/cm^3) WC (Ø 0.79 mm; 14.7 g/cm^3)	T91 (Ø 0.1 mm; 7.9 g/cm^3)

times and this due to its higher rotation speed up to 1100 rpm. Conventional planetary ball-milling is limited to 800 rpm. By increased rotation speed, the kinetic energy of the grinding bodies is consequently increased with 150%. The higher rotation speed of the nano-premium line system is created by the different way in which the grinding bowls clamp or sink on/into the sun disk, respectively. In the case of a regular conventional mill the bowls clamp onto the sun disk. In case of the nano-mill device, the bowls sink into it, fastening the grinding bowls onto the sun disk and counter rotating them around its centre.

The milling process parameters are listed in Table 2. The maximal rotational speeds achieved in practice were 626 and 1000 rpm, respectively. Suspension concentration, milling time and grinding media were varied. The influence of the grinding media (diameter and materials type) on the particle size distribution (PSD) was investigated.

As primary grinding medium, spherical Y_2O_3 stabilized zirconium oxide beads (YSZ, Gimex Technical Ceramics BV, the Netherlands, diameter 3 and 10 mm) were used for conventional planetary ball-milling. Stainless steel beads (SS, Fritsch GmbH, Germany, 1 mm diameter) were used as primary beads in the case of nano-milling. After the particle size was reduced to submicron level using conventional as well as nano-milling, secondary grinding beads were loaded in the system in order to implement an extended particle break-up to nano-level. High-chromium steel powder (T91,[2] ArcelorMittal Research Industry Gent, diameter 0.1 mm) and tungsten carbide beads (Glen Mills, WC, USA, 0.79 mm) were used as secondary grinding medium in the system. A Mastersizer X (Malvern Instruments Ltd., United Kingdom) was used in order to determine the PSD of the T91 powder before and after nano-milling and to verify if the broken particles were not mixed with the T91 powder. To verify progress in powder milling, PSD's before and after desagglomeration were determined using particle size disc centrifuging or CPS. D_{10}, D_{50} and D_{90} are the statistical fractions determined basically on the cumulative frequency curve.

After preparing a suspension concentration, the primary grinding medium (400 g YSZ beads, sized 3 mm) was added to the suspension. After, the suspension was milled at a rotation speed of 626 rpm. Suspension pre-milling was done with yttria stabilized zirconia (YSZ) for effective milling times of 6 h. After pre-milling, the secondary grinding medium (60 g WC beads, diameter 0.79 mm) was added. Additional effective milling was done for another 155 min.

In order to be sure that the observed PSD is only determined by the nano-yttrium oxides particles, as mixing of beads can cause wear, the size of the T91 powder before and after nano-milling has been verified using centrifugal particle sizing (CPS). As the distribution of the T91 powder is measured to be outside the CPS detection range of 2–100 nm, it can be concluded that the detected PSD values can be ascribed to the suspended nano-particles and that the remaining T91 powder is still micron-sized. Therefore, for ζ-potential and viscosity measurements the suspensions were used after eye-verification of the sinking down of the T91 material.

2.3. Suspension characterization

2.3.1. Zeta potential titrations

Titrations in the basic region using 5 M KOH on as-received yttria (Y_2O_3) powder suspensions were done in order to evaluate the evolution of ζ-potential value of the colloidal system in the basic pH, with and without the addition of the dispersant Calgon N. For ζ-potential titrations, a standard 0.6 vol.% Y_2O_3 suspension was prepared for studying the ζ-potential of the as-received powder suspension in the basic region without dispersant addition using 5 M KOH solution. A 2 vol.% aqueous Y_2O_3 suspension was prepared using ball-milling, in order to verify the evolution of ζ-potential after dispersant addition. In both cases distilled water was used as suspension medium.

2.3.2. Dispersant coated particles

Transmission electron microscopy (TEM) was used for visualization of the dispersion after Calgon N addition for a 0.6 vol.% as-received yttria (Y_2O_3) powder suspension and a 2 vol.% suspension prepared using planetary ball-milling. TEM samples were prepared by the suspension drop method with the use of lacey carbon grids (Electron Microscopy Sciences, United Kingdom): a drop has been taken after particle surface modification and was dripped manually onto the carbon grid. The particle observations were made using a TEM JEOL JEM 3010 equipment (JEOL).

[2] enflaCERI 4812S0272-8842(11)00997-7.

2.3.3. Suspension rheology

In order to determine the optimal dispersant concentration, the rheological properties were investigated at 25 °C using a rotational rheometer (MARS II, Thermo Electron, Germany) at shear rates ranging from 1 to 1000 s^{-1}. All un-milled suspensions contained 4 vol.% Y_2O_3 of solid loading. The milled suspension was diluted to a 1 vol.% concentration, as the undiluted system appeared too viscous to be workable. In all cases Calgon N was added in order to stabilize the dispersion.

3. Results and discussion

3.1. Powder characterization

Fig. 1 shows the relative weight percentage (rel. wt.%) as a function of particle size distribution (PSD) as well as the cumulative frequency curve of the as-received yttria (Y_2O_3) powder, characterized by its statistical fractions D_{10}, D_{50} and D_{90} with a value of 0.142, 0.402 and 0.734 μm, respectively.

From this data it can be concluded that the in-batch Y_2O_3 particle population is bimodal agglomerated containing an agglomerate fraction in the submicron range (∼500 nm) and a fraction sized above 1 μm. A micrograph of the as-received powder obtained using scanning electron microscopy (SEM) is presented in Fig. 2, confirming the agglomeration state of the individual nano-particles as well as their spherical morphology in the as-received distribution.

3.2. Suspension preparation

3.2.1. Dispersant selection

Fig. 3 illustrates the ζ-potential value as a function of dispersing agent's volume added to a 0.6 vol.% yttria (Y_2O_3) suspension. Fig. 3 illustrates that Y_2O_3 particles suspended in water exhibit a positive surface charge of about +30 mV. Depending on the consulted literature source, an absolute surface charge value of approximately |30 mV| should be sufficient to create a stable suspension based on inter-particle

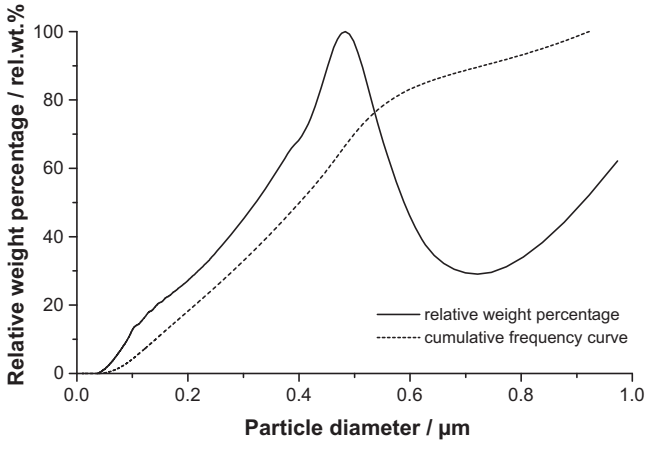

Fig. 1. Relative weight percentage (rel. wt.%) and cumulative frequency curve as a function of particle diameter for the yttria (Y_2O_3) powder in the as-received condition.

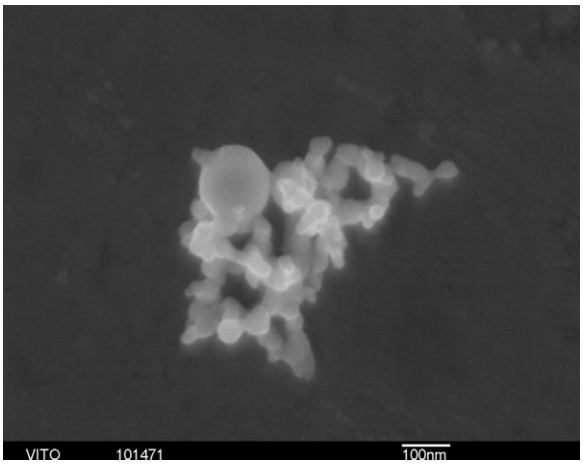

Fig. 2. Scanning electron micrograph (SEM) of the yttria (Y_2O_3) powder in the as-received state.

electrostatic repulsions. However, electrostatic repulsion is a rather weak force, which will not avoid that in time particle re-agglomeration will take place. Therefore, in order to prepare stable Y_2O_3 nano-dispersions withstanding time, it is important to keep the Y_2O_3 suspensions homogeneously dispersed after particle break-up by preventing this re-agglomeration.

From Fig. 3, it is observed that Calgon N, being a negatively charged dispersant, adsorbs on the surface of the yttria (Y_2O_3) particles, rendering the ζ-potential negative. When added in sufficient amounts, the surface of the Y_2O_3 is completely covered with Calgon N, resulting in a ζ-potential of about −30 mV. In order to keep the dilution of the colloidal suspension minimal, the most efficient dispersing agent is that for which the lowest volume of dispersant has to be added to reach the point of stabilization of about −30 mV. As such, with Calgon N a minimal loss in suspension concentration is achieved which is required for its practical application (c_{ini} = 0.6 vol.%; c_{end} = 0.5 vol.%).

3.2.2. Particle size reduction

Particle size distributions (PSD's) of yttria (Y_2O_3) nano-powders in the as-received state are in reality often submicron or even supermicron agglomerated. To date, production of

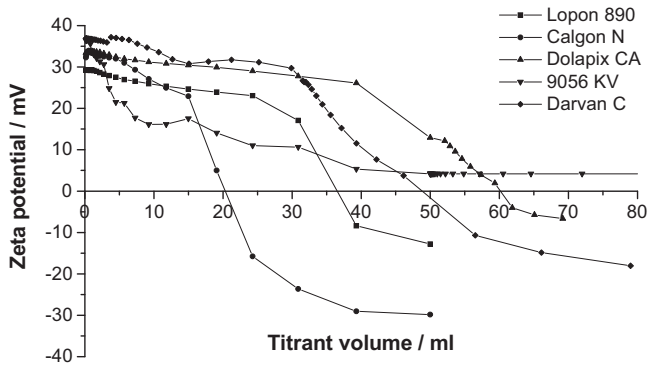

Fig. 3. ζ-Potential value as a function of total titrant volume added to a 0.6 vol.% yttria (Y_2O_3) suspension for different dispersing agents tested.

powders is yet possible in bulk quantities but mostly still consisting of significant and harsh agglomerated particle populations [20]. For the Y_2O_3 powder used in our study, the discrepancy between commercial offered size and the real agglomerated particle size was confirmed with centrifugal particle sizing (CPS), as demonstrated in Fig. 1. To reach the desired PSD in terms of fine sized (<100 nm) and non-agglomerated powder, it was necessary to implement a particle break-up of the as-received Y_2O_3 powder.

3.2.2.1. Nano-milling. Fig. 4 illustrates the reduction in particle size (D_{10}, D_{50} and D_{90}) achieved using nano-milling for a 2 vol.% yttria (Y_2O_3) suspension as a function of ball-milling time. As primary grinding medium, 1 mm diameter spherical stainless steel beads were used. In order to verify the effect of a secondary grinding media addition onto particle size reduction, T91 powder was added at the start-run of milling as well as after submicron break-up (i.e. after 6 min nano-milling).

Considering Fig. 4, it can be concluded that the addition of finest secondary T91 powder at start-run has especially an influence on the statistical fraction D_{10} in the beginning of the milling process. It is well known that smaller grinding beads have a lower impact on larger powder particles as they do not have sufficient mass to grind larger powder lumps to smaller sizes. The evolutional trend in D_{50} and D_{90} is mainly due to particle size reduction caused by the bigger grinding beads. The finest particle size distribution achieved within reduced milling time, i.e. after 8 min high-energy nano-milling, is in case when T91 was added at the start of the run and is characterized by a D_{10}, D_{50} and D_{90} of 10, 100 and 400 nm, respectively. Larger milling times do not lead to further size reduction. In case when T91 was added after 6 min of ball-milling the statistical fractions D_{10}, D_{50} and D_{90} are 70, 150 and 300 nm, respectively after 8 min of ball-milling. Extended milling times will be needed in order to reach the same sub-100 nm level in the second case compared to the situation when T91 was added at start-run.

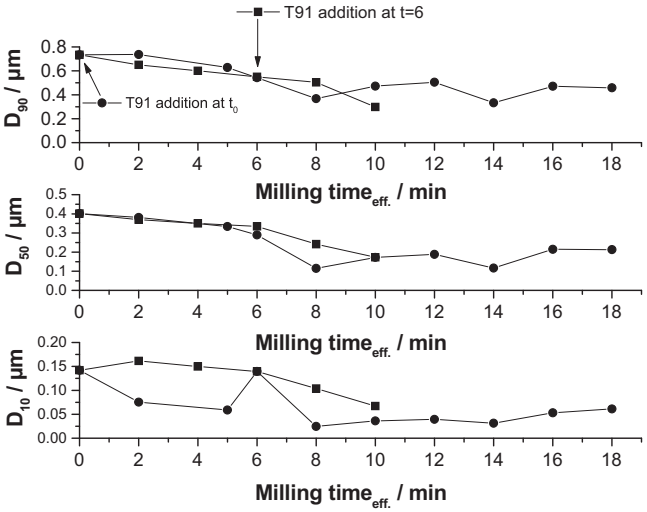

Fig. 4. Particle size statistical fractions D_{10},D_{50} and D_{90} as a function of ball-mill time obtained using advanced nano-milling of a 2 vol.% yttria suspension. Primary grinding medium: 1 mm RVS balls. Secondary grinding media: T91 powder.

In order to be sure that the observed PSD only consists of the nano-sized Y_2O_3 particles, as mixing of beads can cause wear, the size of the T91 powder before and after nano-milling was determined. As the distribution of the T91 powder was measured to be outside the CPS detection range, it can be sure that the PSD values detected can be ascribed to the nano-particles suspension.

3.2.2.2. Conventional planetary milling. After four hours planetary ball-milling with YSZ as primary grinding medium, the yttria (Y_2O_3) powder is broken down to submicron level, ~0.3 μm. T91 powder as well as tungsten carbide (WC) beads

Table 3
Fraction values D_{10}, D_{50} and D_{90} in nanometre (nm) at the most optimal ball-mill time in hours (h) for 2, 3 and 4 volume percentage (vol.%) suspensions. Calculations are based on the relative weight percentage (rel. wt.%) distribution and particle number (rel. p.n.%) versus particle size.

Suspension (vol.%)	Primary grinding media	Secondary grinding media	Milling time (h)	Calculation based on rel. wt.% or rel. p.n.%	D_{10} (nm)	D_{50} (nm)	D_{90} (nm)
2	YSZ, 3 mm	T91, 0.1 mm	4.1	wt.%	32	104	384
2	YSZ, 3 mm	WC, 0.79 mm	5.2	wt.%	39	221	517
3	YSZ, 3 mm	WC, 0.79 mm	6.5	wt.%	25	115	287
4	YSZ, 3 mm	WC, 0.79 mm	5.3	wt.%	55	176	416
2	YSZ, 10 mm	T91, 0.1 mm	4.5	p.n.%	39	212	497
2	YSZ, 10 mm	WC, 0.79 mm	4.5	p.n.%	44	252	484
3	YSZ, 10 mm	WC, 0.79 mm	6.1	p.n.%	45	235	446
4	YSZ, 10 mm	WC, 0.79 mm	3.9	p.n.%	58	225	552
2	YSZ, 3 mm	T91, 0.1 mm	4.1	wt.%	11	17	41
2	YSZ, 3 mm	WC, 0.79 mm	5.2	wt.%	12	14	28
3	YSZ, 3 mm	WC, 0.79 mm	6.5	wt.%	10	13	26
4	YSZ, 3 mm	WC, 0.79 mm	5.3	wt.%	14	27	64
2	YSZ, 10 mm	T91, 0.1 mm	4.5	p.n.%	11	17	36
2	YSZ, 10 mm	WC, 0.79 mm	4.5	p.n.%	12	17	34
3	YSZ, 10 mm	WC, 0.79 mm	6.1	p.n.%	12	17	34
4	YSZ, 10 mm	WC, 0.79 mm	3.9	p.n.%	13	19	45

Note: rel. p.n.%, relative particle number percentage; rel. wt.%, relative weight percentage.

were added to the Y_2O_3 suspension after pre-reduction to submicron level, i.e. exactly after 4 h pre-milling with Y_2O_3 stabilized ZrO_2 (YSZ) beads.

Table 3 depicts the fraction values D_{10}, D_{50} and D_{90} in nanometre (nm) at the most optimal ball-mill time in hours (h) for 2, 3 and 4 volume percentage (vol.%) suspensions. Calculations are based on the relative weight percentage (rel. wt.%) distribution and particle number (p.n.) versus particle size. Primary grinding media used are 3 and 10 mm YSZ beads, secondary grinding beads used are 100 μm T91 powder and 0.79 mm WC beads.

From Table 3 it can be concluded that in case secondary grinding medium (T91 powder) was added, the most efficient size reduction to values ∼104 nm is achieved after 4.1 h of ball-mill time. In the case WC beads were added, a size of 115 nm is reached after 6.5 h of grinding. Furthermore, it can be concluded that in the case 10 mm primary beads were used, the final particle size cannot be reduced below 200 nm. Consequently, the most optimal size reduction is achieved when 3 mm beads were used as primary grinding medium.

The same reduction to approximately 100 nm was achieved during nano-milling, leading to the conclusion that this is probably the maximum agglomeration reduction capacity intrinsic for this specific Y_2O_3 powder, independently of the grinding medium used.

When observing the statistical fractions in relative particle number percentage (rel. p.n.%) as a function of size, it has to be considered that most probably only a minority of Y_2O_3 agglomerated lumps make the curve of the relative weight fraction as a function of particle size move to higher average size values, and that the smallest particles (<50 nm) are statistical representative for the majority of particle population. The biggest advantage of nano-milling compared to conventional planetary milling is definitely its reduced operation time in order to obtain similar particle sizes.

Further size reduction down to (sub)-100 nm level could be tried by adding smaller sized grinding media. Density, material type and size of the grinding medium could be used to implement further reduction. The advantage or disadvantage in using one grinding medium compared to another can be found in its size reduction (submicron particles can only be reduced in size with smaller grinding media), extra milling processing time and in the wear properties of the grinding beads being detrimental for the elemental contamination of the nano-sized suspension [21].

3.2.3. Suspension characterization

In the previous paragraphs particle size reduction was demonstrated using nano-milling and conventional planetary ball-milling. In both cases the final size reduction of the yttria (Y_2O_3) powder investigated in this study appears to be 100 nm. In the following paragraphs and according to the results presented in Figs. 5–11, final particle size reduction is performed using conventional ball-milling. The most optimal conditions concerning milling time and milling media observed in previous paragraphs are used. In all cases distilled water was used as suspension medium. After preparing a suspension

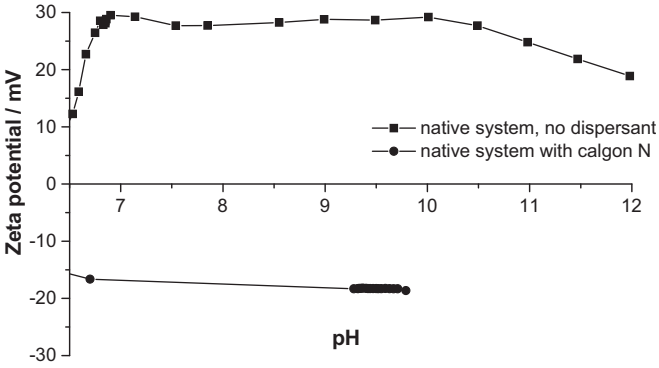

Fig. 5. ζ-Potential as a function of pH obtained during basic titration of a 0.6 vol.% yttria (Y_2O_3) system; both Y_2O_3 suspensions titrated in the as-received condition, with and without Calgon N addition.

concentration of 3 vol.%, the primary grinding medium (400 g YSZ beads, sized 3 mm) was added to the suspension. After, the suspension is milled at a rotation speed of 626 rpm. Suspension pre-milling is done with yttria stabilized zirconia (YSZ) for effective milling times of 6 h. After pre-milling, the secondary grinding medium (60 g WC beads, diameter 0.79 mm) is added. Additional effective milling was done for another 155 min.

3.2.3.1. Zeta-potential titrations. Basic titrations with 5 M KOH were carried out in order to evaluate the evolution in ζ-potential of the colloidal system [nano-particles/dispersant/dispersing medium] compared to the system without dispersant. Fig. 5 presents the ζ-potential as a function of pH for a 0.6 vol.% yttria (Y_2O_3) colloidal system with and without Calgon N addition.

Fig. 5 leads to the conclusion that for the system without dispersant added, the ζ-potential of the as-received Y_2O_3 suspension remains positive over the complete pH range, i.e. from 6.5 to 10. Due to the absence of an IEP for the system in the basic pH region when no dispersant is added, no pH shift in

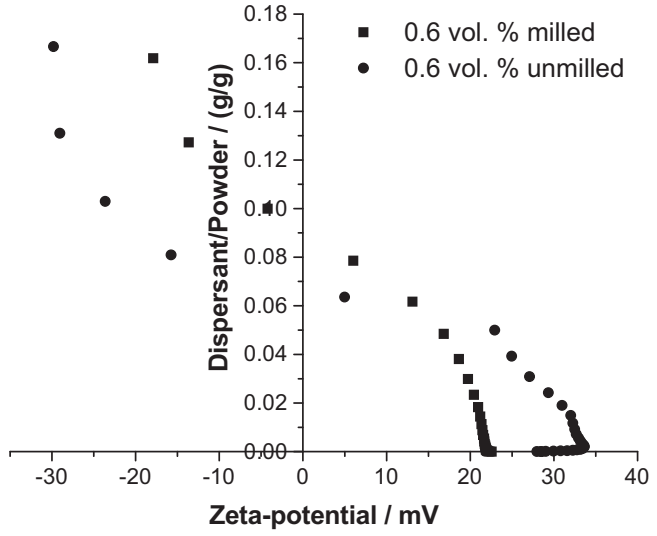

Fig. 6. ζ-Potential value as a function of total titrant volume added for 0.6 vol.% milled and un-milled yttria suspensions titrated with Calgon N.

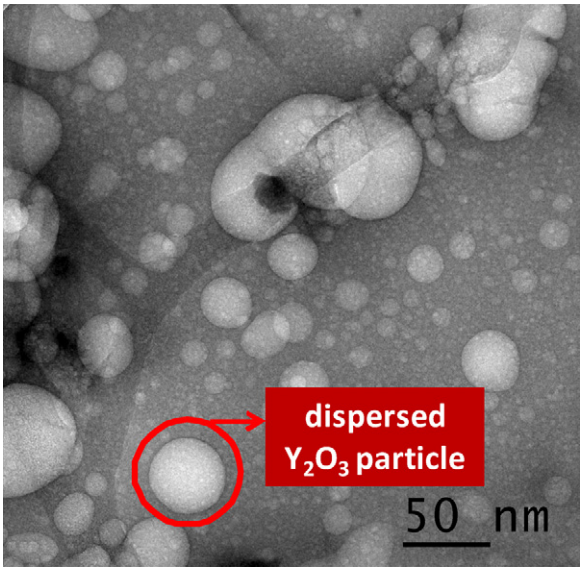

Fig. 7. Transmission electron micrograph (TEM) of coated yttria (Y_2O_3) nanoparticles, with indication of a coated Y_2O_3 particle on image.

the IEP is detected after dispersant addition. After addition of the negatively charge dispersant, the ζ-potential is shifted to −20 mV in the pH range of 6–10, confirming the adsorption and stability of the dispersant adsorption in that pH region.

In conclusion of this section, it can be stated that it is possible to achieve a stable suspension in the pH range from 6 to 10.

3.2.3.2. Dispersant coated particles. The ζ-potential value as a function of total titrant volume added was determined for a 0.6 vol.% yttria (Y_2O_3) powder suspension in the un-milled as well as in the milled condition and is presented in Fig. 6.

Fig. 6 reveals that the ratio of dispersant/powder (g/g) is higher after ball-milling compared to a suspension prepared with as-received powder. This can be understood by the fact that more dispersant is needed after ball-milling as the available area highly increases after particle size reduction. Based on the experimental results obtained, the amount of dispersant needed

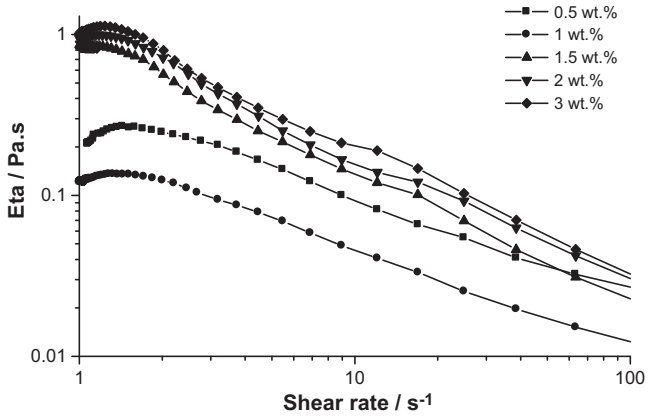

Fig. 8. Dynamic viscosity (η_0) as a function of shear rate (s^{-1}) for a 4 vol.% solid loads in the un-milled powder condition and under the addition of 0.5–3 wt.% of dispersant Calgon N.

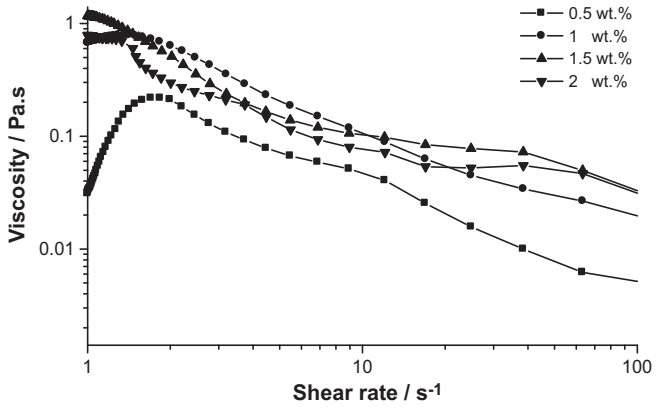

Fig. 9. Dynamic viscosity (η_0) as a function of shear rate (s^{-1}) for a 0.7 vol.% solid load in the ball-milled powder condition and under the addition of 0.5–3 wt.% dispersant Calgon N.

to stabilize the colloidal dispersions can be deduced in grams per gram Y_2O_3 powder to be dispersed.

Fig. 7 represents a transmission electron micrograph (TEM) of the Y_2O_3 powder dispersed with Calgon N dispersant, under excess addition of dispersant.

From the TEM image presented in Fig. 7 it can be concluded that coating of the Y_2O_3 particles based on electrosteric stabilization appears to be possible.

3.2.3.3. Suspension rheology. The dynamic viscosity (η) as a function of shear rate (s^{-1}) under different dispersant additions for 4 and 0.7 vol.% yttria (Y_2O_3) solid loads in the un-milled and milled condition are plotted in Figs. 8 and 9, respectively.

Depending on the suspension composition and stability, different flow types can be distinguished under steady shear regime. When viscosity behaves independent of the shear rate, the flow behaviour is denominated Newtonian flow. Shear-thinning response is observed for all Y_2O_3 suspensions studied.

Fig. 10 presents the suspension's dynamic viscosity as a function of dispersant concentration added at a constant shear rate of 4 s^{-1} for the as-received Y_2O_3 powder (4 vol.%) as well as after ball-milling a 1 vol.% suspension.

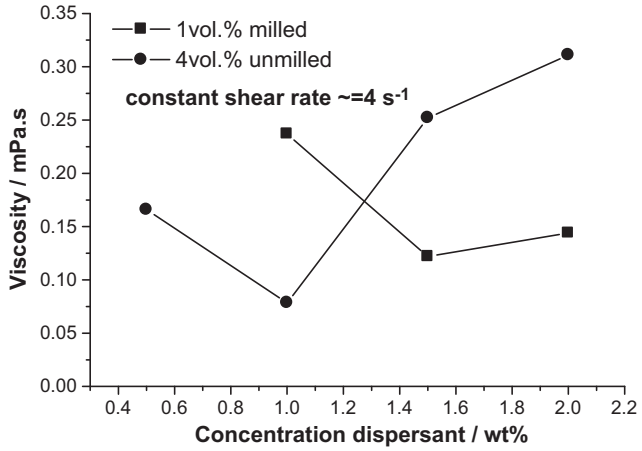

Fig. 10. Viscosity (η_0) as a function of added dispersant concentration (wt.%) at constant shear rate of 4 s^{-1} for a 4 vol.% un-milled yttria (Y_2O_3) powder suspension as well as under milling conditions (1 vol.%).

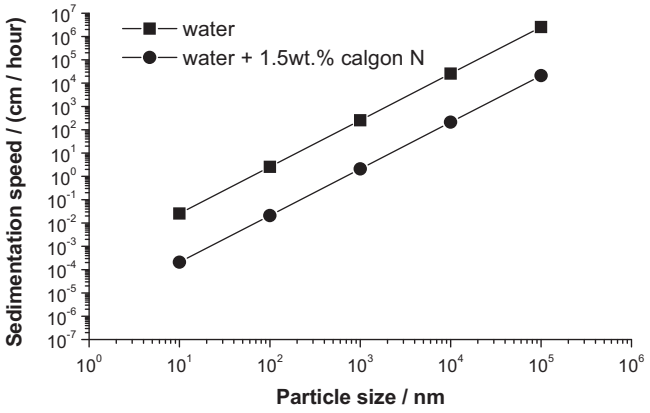

Fig. 11. Sedimentation rate (v) as a function of particle size calculated using the law of Stokes for individual particles sinking out in dispersion media water and water with 1.5 wt.% Calgon N addition.

From Fig. 10, it can be concluded that the amount of dispersant addition has an influence on the viscosity and that the optimal dispersant concentration to achieve low-viscous suspensions increases from 1 to 1.5 wt.% for as-received powder and ball-milled suspensions, respectively. Decreased particle size increases the particles specific surface area (SSA), leading to increased dispersant addition needed after milling in order to obtain minimal suspension viscosity.

3.2.3.4. Suspension life-time. For practical manipulations, suspension stability in terms of time to sink down to the bottom of the vial is of interest. According to the law of Stokes, the rate of creaming (v) or sedimentation of individual particles < 100 μm follows Eq. (1) [22]. The parameters a, ρ_p, ρ_l, g and η_0, represent particle size, particle density, density of the dispersion medium and dynamic viscosity of the dispersion medium, respectively. The parameter g is the constant of gravity. The particles density, density and dynamic viscosity of the dispersion medium with and without dispersant addition Calgon N are $\rho_{Y_2O_3} = 5.01\,g/cm^3$, $\rho_{H_2O} = 1\,g/cm^3$, $\eta_{H_2O} = 1$ mPa s and $\eta_{H_2O+DISP} = 122$ mPa s respectively. The η_0-value (122 mPa s) of the system after Calgon N addition was based on the viscosity curve minimum observed in Section 3.2.3.3.

$$v = 2a^2|\rho_p - \rho_l|g\frac{9}{\eta_0} \quad (1)$$

Following the law of Stokes, the rate of sedimentation or creaming may be diminished by reduction in particle size (nano-sized suspensions) and by increasing the viscosity using a dispersant. Sedimentation time as a function of particle size is presented in Fig. 11. The values presented in Fig. 11 are singular points calculated from the law of Stokes.

From Fig. 11, it can be concluded that the system with dispersant addition increases in stability compared to the colloidal system consisting of only the dispersion medium water. After 1.5 wt.% Calgon N addition, colloidal stability increases with approximately 10^2 h. After 48 h, 100 nm sized particles will flocculate to the bottom of the vial.

4. Conclusion

A formulation for the preparation of low-viscous and low-loaded (2, 3 and 4 vol.%) nano-sized yttria (Y_2O_3) colloidal suspensions is proposed within this work. This study enlightens the path for simple and robust preparing of such colloidal systems: powder characterization, suspension preparation and low-load slurry characterization.

The Y_2O_3 powder in its as-received state appears to be submicron agglomerated and needs ball-milling in order to reduce the as-received particle distribution down to the nano-level. After screening several electrosteric dispersants, Calgon N appears to be a potential dispersant applied in this study, inducing minimal suspension dilution.

In this study, particle size reduction was achieved using conventional planetary ball-milling and compared to advanced high energetic nano-milling systems. The nano-mill Pulverisette 7 was presented here as an excellent possibility to produce particle suspensions in the nanometre range within reasonably low milling times. The new planetary ball-mill generation Fritsch Pulverisette 7, 6 and 5 premium line is demonstrated by the producer to be the new standard for the creation of nano-powders on a lab-scale: faster, simpler and safer communication to nano-level. With the Fritsch P-7 Pulverisette, (sub)-100 nm distributions are procured considerably faster compared to conventional planetary milling, in case of appropriate dispersant selection and low-solid loads preparation, which also prevents strong agglomeration. Using nano-milling, a powder suspension can be milled down to nano-level within reduced reaction time compared to conventional planetary ball-milling. The ζ-potential of as-received Y_2O_3 nano-sized suspensions remains positive and in the absence of an isoelectrical point (IEP) over the complete pH range of 6.5–10. There is no IEP detection for as-received Y_2O_3 nano-powders in the basic pH region. The minimum in the curve dynamic viscosity as a function of concentration of dispersant increases significantly from 1 to 1.5 wt.% dispersant addition in the case of the as-received Y_2O_3 powder suspension and the ball-milled suspension, respectively. Colloidal life-time was approached using the law of Stokes. It can be concluded that after dispersant addition Calgon N (1.5 wt.%), colloidal life-time increases with 10^2 h.

Acknowledgements

Ghent University and ArcelorMittal Research Industry Ghent (OCAS) are thanked for academic and financial support. VITO is gratefully acknowledged for providing the experimental equipment, as well as the numerous discussions, with a special thanks to A.-M. De Wilde, I. Thijs, M. Schroeven and R. Kemps. The microstructure group of SCK·CEN is thanked for TEM equipment service.

References

[1] F.A. Cotton, G. Wilkinson, Advanced Inorganic Chemistry, 5th ed., John Wiley & Sons, New York, 1988;
A.R. West, Solid State Chemistry and its Applications, John Wiley & Sons, New York, 1984.

[2] G. Adachi, N. Imanaka, Chem. Rev. 98 (1998), 1479, plus references herein.
[3] G. Adachi, Science of Rare Earths, Kagaku-dojinn, Kyoto, 1999.
[4] J.G. Bednorz, K.A. Müller, Z. Phys. B64 (1986) 189.
[5] J.H. Lunsford, Angew. Chem. Int. Ed. Engl. 34 (1995) 970.
[6] M.J. Capitan, P. Malet, M.A. Centeno, A. Munoz-Paez, I. Carrizosa, J.A. Odriozola, J. Phys. Chem. 97 (1993) 9233.
[7] R.L. Kleuh, D.R. Harries, High-chromium ferritic and martensitic steels for nuclear applications, ASTM Stock Number: MONO3, ISBN 0-8031-2090-7, version 2001.
[8] K. Verhiest, A. Almazouzi, N. DeWispelaere, R. Petrov, S. Claessens, Development of oxides dispersion strengthened steels for high temperature nuclear reactor applications, J. Nucl. Mater. 385 (2) (2009) 308–311.
[9] C. Capdevilla, H.K.D.H. Bhadeshia, Manufacturing and microstructural evolution of mechanically alloyed oxide dispersion strengthened superalloys, Adv. Eng. Mater. 3 (9) (2001).
[10] Literature Study on Ferritic ODS steels for HTapplications, N. Baluc, Final Report on the EFDA Task TW4-TTMW-006 Deliverable 2, (2004).
[11] F.F. Lange, Powder processing science and technology for increased reliability, J. Am. Ceram. Soc. 72 (1989) 3–15.
[12] T.F. Tadros, Industrial applications of dispersions, Adv. Colloid Interface Sci. 46 (1993) 1–47.
[13] C.A. Traina, S. Jeffrey, Surface modification of Y_2O_3 nanoparticles, Langmuir 23 (2007) 9158–9161.
[14] Y. Kuroda, H. Hamano, T. Mori, Y. Yoshikawa, M. Nagao, Specific adsorption behavior of water on a Y_2O_3 surface, Langmuir 16 (2000) 6937–6948.
[15] M.K.M. Hruschka, W. Si, S. Tosatti, T.J. Graule, L.J. Gauckler, Processing of beta-silicon nitride from water-based alfa-silicon nitride, alumina, and yttria powder suspensions, J. Am. Ceram. Soc. 82 (8) (1999) 2039–2043.
[16] C. Takai, M. Tsukamoto, M. Fuji, M. Takashashi, Control of high solid content yttria slurry with low viscosity for gelcasting, J. Alloys Compd. 408–412 (2006) 533–537.
[17] G. Bernard-Granger, C. Guizard, Sintering behavior and optical properties of yttria, J. Am. Ceram. Soc. 90 (9) (2007) 2698–2702.
[18] F.F. Lange, Powder processing science and technology for increased reliability, J. Am. Ceram. Soc. 72 (1) (1989) 3–15.
[19] A.J. Lewis, Colloidal processing of ceramics, J. Am. Ceram. Soc. 83 (10) (2000) 2341–2359.
[20] I. Santacruz, M.I. Nieto, J. Binner, R. Moreno, Gel casting of aqueous suspensions of $BaTiO_3$ nano powders, Ceram. Int. 35 (2009) 321–326.
[21] J.R. Sneeringer, Selecting the right ceramic media for high-energy mills, Am. Ceram. Soc. Bull. 80 (10) (2001) 49–51.
[22] Seminar on Dispersions and Emulsions: Formation, Stabilisation and Characterization, organized by the Belgian Particle, Colloid and Interface Society (BEPCIS), June 8–10, Sint-Martens-Latem, 2009.